

## Ligustilide counteracts carcinogenesis and hepatocellular carcinoma cell-evoked macrophage M2 polarization by regulating yes-associated protein-mediated interleukin-6 secretion

Jikang Yang<sup>1</sup> and Zhiyuan Xing<sup>2</sup> 

<sup>1</sup>Department of Gastroenterology, Jiaozuo People's Hospital, Jiaozuo 454000, China; <sup>2</sup>Emergency Department, Jiaozuo Hospital of Traditional Chinese Medicine, Jiaozuo 454150, China

Corresponding author: Zhiyuan Xing. Email: xingzhiyu@163.com

### Impact statement

Hepatocellular carcinoma (HCC) constitutes the overwhelming majority of liver cancer, and cross-communication between cancer cells and macrophages within the tumor microenvironment fulfills critical roles in the progression of cancer, including HCC. In this study, our findings corroborated that ligustilide not only inhibited HCC cell malignancy but also antagonized macrophage recruitment and M2 polarization evoked by HCC cells via inhibition of yes-associated protein (YAP)/interleukin-6 (IL-6) release-induced activation of the IL-6R/signal transducer and activator of transcription 3 (STAT3) signaling. Thus, this is the first study to confirm that ligustilide may attenuate the progression of HCC by regulating cancer cell malignancy and the interplay between the tumor cells and macrophages in the tumor microenvironment, supporting a potential therapeutic agent that can complement and optimize available therapeutic strategy against HCC.

### Abstract

Cross-communication between cancer cells and macrophages within the tumor microenvironment fulfills the critical roles in the progression of cancers, including hepatocellular carcinoma (HCC). Ligustilide exerts anti-inflammation, anti-injury, and anti-tumor pleiotropic pharmacological functions. Nevertheless, its roles in HCC cells and tumor microenvironment remain elusive. In the current study, ligustilide dramatically restrained HCC cell viability and migration but had little cytotoxicity to normal hepatocytes. Importantly, ligustilide antagonized HCC cell co-culture-induced macrophage recruitment and M2 polarization by enhancing the percentage of CD14<sup>+</sup>CD206<sup>+</sup> cells and macrophage M2 markers (CD163, Arg1, CD206, CCL22, IL-10, and TGF- $\beta$ ). Mechanistically, ligustilide repressed yes-associated protein (YAP) activation by reducing nuclear translocation, protein expression, transcriptional regulatory activity of YAP, and increasing p-YAP levels. Noticeably, blocking the YAP offset the suppressive effects of ligustilide on macrophage recruitment and M2 polarization evoked by HCC cells. Moreover, the release of interleukin-6 (IL-6) was mitigated by ligustilide in a YAP-dependent manner in HCC cells, concomitant with inhibition of IL-6R/STAT3 signaling activation. Of interest, interdicting the IL-6 aggravated ligustilide-mediated suppression in HCC-induced macrophage recruitment and M2 polarization; whereas exogenous IL-6 treatment reversed the above effects. Additionally, blockade of IL-6R signaling also overturned IL-6-induced macrophage recruitment and M2 phenotype. Consequently, these findings support a notion that ligustilide not only restrains HCC cell malignancy but also antagonizes HCC cell-evoked macrophage recruitment and M2 polarization by inhibiting YAP/IL-6 release-induced activation of the IL-6 receptor/signal transducer and activator of transcription 3 (IL-6R/STAT3) signaling. Thus, ligustilide may be a promising therapeutic agent to fight HCC by regulating cancer cells and cross-talk between tumor cells and macrophages in tumor microenvironment.

**Keywords:** Hepatocellular carcinoma, tumor microenvironment, ligustilide, macrophage recruitment, macrophage polarization

*Experimental Biology and Medicine* 2021; 246: 1928–1937. DOI: 10.1177/15353702211010420

### Introduction

Liver cancer currently ranks as the sixth most prevalent cancer in incidence and causes 782,000 deaths annually.<sup>1</sup> Hepatocellular carcinoma (HCC) appropriates the overwhelming majority of liver cancers (comprising

approximately 90% of cases) and is a frequently occurring and aggressive malignancy that typically develops as a sequel to protracted chronic liver disease or cirrhosis.<sup>2</sup> Epidemiological investigation confirms a rising incidence and mortality of HCC, a primary liver tumor, in

North America, European regions, and Asia,<sup>3,4</sup> and corroborates that HCC leads to the fourth-highest number of deaths annually worldwide.<sup>2,4</sup> Due to the great advances in traditional interventions of surgery resection, transplantation, chemotherapy, and immunotherapy, patients with early-stage HCC usually achieve encouraging results in terms of both safety and efficacy from these strategies. Nevertheless, a majority of patients with HCC are diagnosed at an advanced stage, and are highly resistant to the current curative treatment options, resulting in 70% tumor recurrence within five years.<sup>2,5</sup> Thus, novel therapeutic approaches are urgently needed for the treatment of HCC.

Traditional research has mainly focused on the direct regulation of cancer cell malignant behavior, such as cell proliferation and invasion. Noticeably, increasing evidence supports a critical role of tumor microenvironment (TME) in the initiation and progression of cancers including HCC.<sup>6-8</sup> Actually, TME usually refers to the environment where tumor cell exists and includes many stromal cells, such as fibroblast and macrophages. Among them, tumor-associated macrophages (TAM) are the abundant and major components within the TME and exhibit great phenotypic heterogeneity.<sup>9,10</sup> Epidemiological investigation reveals a positive relationship between high densities of TAM and poor prognosis in HCC patients.<sup>11</sup> In fact, TAM usually

originate from circulating monocytes and can be recruited within the TME by tumor cell-derived extracellular signals that may educate TAM from tumoricidal M1 phenotype to pro-tumor M2 phenotype; while macrophages will in turn affect tumor growth and the evolution of tumor cells.<sup>6,12,13</sup> The cross-talk between cancer cells and TAM can drive malignancy and therapy failure, including that of HCC.<sup>11,14</sup> Remarkably, driving macrophage M2 polarization may facilitate the development of HCC and metastasis *in vivo* by regulating cell viability, invasion, and migration.<sup>10,14</sup> Currently, deciphering the mechanism lying beneath the interaction between HCC cells and TAM is a novel therapeutic strategy against HCC.<sup>14</sup>

Ligustilide (Figure 1(a)) is a proverbial and natural bio-active benzoquinone derivative extracted from Chinese herbal medicines, such as *Radix Angelica Sinensis* that has been used to alleviate various diseases syndromes for over a thousand years. Multiple studies have corroborated that ligustilide exerts broad pharmaceutical applications in various diseases, such as cardiovascular disease,<sup>15</sup> brain injury, and inflammation.<sup>16</sup> Increasing evidence reveals the critical roles of ligustilide in the progression of several carcinomas, including ovarian cancer,<sup>17</sup> breast cancer,<sup>18</sup> melanoma,<sup>19</sup> and glioma.<sup>20</sup> For instance, administration with ligustilide restrains the migration of glioma cells.<sup>20</sup> Noticeably, a recent study confirms the pro-apoptotic efficacy of

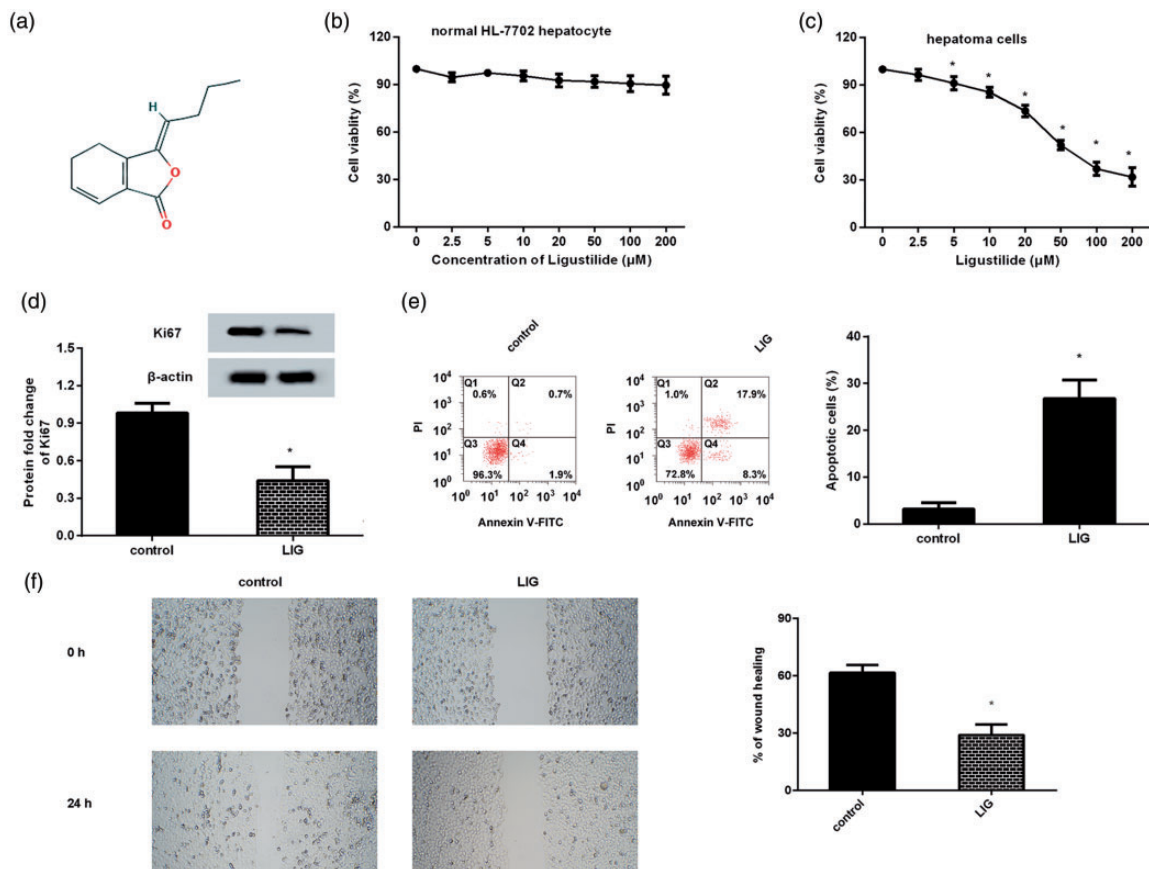


**Figure 1.** Ligustilide mitigated the malignancy of HCC cells. (a) The chemical structure of ligustilide. (b) Cell viability was determined in normal hepatocytes after ligustilide treatment. (c) HCC cell line HepG2 was treated with the indicated doses of ligustilide. Then, CCK-8 assay was used to determine cell viability. (d) The protein expression of proliferation-related Ki67 was analyzed by Western blotting. (e and f) The effects of ligustilide on HCC cell apoptosis (e) and migration (f) were investigated. \* $P < 0.05$  vs. control group. (A color version of this figure is available in the online journal.)

ligustilide in prostate-cancer-associated fibroblast in TME, implying a potential role of ligustilide in prostate cancer progression by affecting TME.<sup>21</sup> However, the roles of ligustilide in HCC remain elusive. In the current research, we sought to investigate the function of ligustilide in HCC cell proliferation, apoptosis, and migration. Additionally, the potential of ligustilide on TME in HCC was also elaborated by exploring its roles in cancer cell-induced macrophage polarization.

## Materials and methods

### Cell lines and cell culture

The human HCC cell line HepG2, monocytic cell line THP-1, and normal human HL-7702 hepatocytes were obtained from the American Type Culture Collection (ATCC; Manassas, VA, USA). For culture, the HepG2 and THP-1 cells were maintained in RPMI medium (Gibco, Grand Island, NY, USA) supplemented with 10% fetal bovine serum (Thermo Fisher Scientific, Waltham, MA, USA) and 100 U/mL penicillin/streptomycin. During this process, cells were kept in a 5% CO<sub>2</sub> incubator with saturated humidity at 37°C.

### Cell counting kit-8 (CCK-8) assay for cell viability

HCC cells and normal human HL-7702 hepatocytes were cultured in a medium containing ligustilide ( $\geq 96\%$  purity; Sigma, St. Louis, MO, USA) ranging from 0 to 200  $\mu\text{mol/L}$ . Approximately 24 h later, cells in each well were further incubated with medium supplemented with 10  $\mu\text{L}$  CCK-8 reagent (Beyotime, Shanghai, China) for 1.5 h. Subsequently, the OD values at 450 nm were determined for assessment of cell viability.

### Cell apoptosis detection

HCC cells were treated with the indicated concentrations of ligustilide. Then, cells were centrifuged, resuspended, and incubated with 5  $\mu\text{L}$  Annexin V-FITC and 10  $\mu\text{L}$  PI (Beyotime). After incubation at room temperature for 15 min in the dark, cells were then subjected to a FACScan flow cytometer (Becton Dickinson, NJ) to analyze cell apoptosis.

### Wound healing assay

Cancer cells were seeded in a 24-well plate and treated with ligustilide. Then, a disposable pipette tip was applied to construct a single scratch wound. After wounding, the non-adherent cells were then removed by rinsing the monolayer of cells using phosphate-buffered saline. Approximately 48 h later, the wounded cultures were photographed by microscopy, and the scratch wound widths were quantified to assess cell migration ability. All experiments were carried out in triplicate.

### Construction of YAP recombinant vector

TRIzol Reagent (Invitrogen, Carlsbad, CA, USA) was applied to extract total RNA from HCC HepG2 cells.

Then, the cDNA was synthesized according to the instructions provided with the SuperScript II First-Strand Synthesis System (Invitrogen). Subsequently, human full-length yes-associated protein (YAP) cDNA was prepared by the PCR application. Subsequently, the YAP cDNA was digested and inserted into the pCDNA3.1(+) plasmid (Invitrogen) to generate a YAP recombinant plasmid (rYAP). Then, 0.5  $\mu\text{g}$  of rYAP vectors or empty vectors were used to transfect HepG2 cells with Lipofectamine 2000 (Invitrogen). The efficacy of YAP expression was evaluated by Western blotting.

### IL-6 receptor (IL-6R) knockdown

To interdict the expression of IL-6R in macrophages, the siRNA sequences targeting IL-6R and the scrambled control (si-con) were bought from Invitrogen. Macrophages derived from THP-1 cells were then transfected with 20 nM siRNA-IL6R or si-con according to the manufacturer's recommendations. Then, the effect on IL-6R expression was evaluated at 48 h post-transfection by Western blotting.

### Co-culture and transwell assay

HCC cells and macrophages co-culture were conducted using a transwell co-culture chamber (Corning, Kennebunk, NY, USA). Briefly, HepG2 cells pre-treated with the indicated doses of ligustilide ( $\geq 96\%$  purity), rYAP plasmids, or exogenous IL-6 (10 ng/mL) were seeded into the upper chamber. Before plating in the bottom chamber, THP-1 monocytes were induced into M0 macrophage by incubation with 100 nM phorbol 12-myristate 13-acetate (PMA, Sigma) for 24 h. Macrophages co-cultured with RPMI medium were introduced as the control group. Approximately 48 h later, the chamber was fixed with 4% paraformaldehyde. Then, 0.1% crystal violet solution was added to stain the migrated cells, followed by photographing under a light microscope ( $\times 100$  magnification).

### Flow cytometric evaluation

To assess macrophage polarization, THP-1 macrophages were collected after co-cultured with HCC cells for 48 h. Then, cells were incubated with fluorescent conjugated anti-human APC-CD14 antibodies (macrophage marker; eBiosciences, San Diego, CA) and FITC-CD206 antibody (M2 macrophage marker). After treatment for 1 h, cells were rinsed and analyzed with a FACScan flow cytometer and Cell Quest software (Becton Dickinson, San Jose, CA) to assess macrophage M2 polarization.

### qRT-PCR assay

The prepared cDNA was applied as an amplified template to perform the real-time PCR using a commercial SYBR Premix Ex Taq<sup>TM</sup> II Kit (TaKaRa, Dalian, China). All protocols were conducted according to the manufacturers' instructions. For quantitation of the transcriptional levels of CD206, CD163, CCL22, Arg1, TGF- $\beta$ , IL-10, YAP, CTGF, and IL-6, the specific oligonucleotide primers for these

genes were synthesized by Shengong Biotechnology Co., Ltd. (Shanghai, China). The PCR reactions were performed on an ABI PRISM 7000 system (Applied Biosystems, Foster City, CA, USA).  $\beta$ -Actin was referred to as an internal control to calculate the relative mRNA expression using the  $2^{-\Delta\Delta C_t}$  method.

### ELISA measurement

After co-culture between M0 macrophages and HCC cells, all cells were collected. Then, the contents of IL-6 in HCC cell supernatants and TGF- $\beta$ , IL-10 in supernatants from macrophages were determined using the commercial ELISA kits (Invitrogen). All procedures were conducted according to manufacturers' instructions.

### Immunoblotting analysis

Cells were lysed with RIPA lysis buffer. The nuclear protein was prepared using a Nuclear Protein Extraction Kit (Beyotime). Then, the bicinchoninic acid (BCA) protein assay kit (Beyotime) was used to determine the isolated protein concentration. Afterward, equal amounts of protein extracts were loaded onto a 12% SDS-PAGE gel and transferred to the polyvinylidene difluoride membrane. Then, membranes were blocked with Tris-buffer saline (TBS) containing 5% non-fat milk and incubated with primary antibodies against Ki67, YAP, p-YAP, Lamin B, IL-6R, signal transducer and activator of transcription 3 (STAT3), and p-STAT3 (all from Abcam, Cambridge, MA, USA) overnight at 4°C. Following extensive washing with TBST, horseradish peroxidase-conjugated secondary antibodies were introduced for further incubation for 2 h. Bound antibodies were then visualized using ECL detection reagent (Millipore, Boston, MA). For normalization, Lamin B was applied for gene expression in nucleus, and  $\beta$ -actin for the expression other genes. A Gel DocTM XR imaging system (Bio-Rad Laboratories, Hercules, CA, USA) and Image J software were used to evaluate protein expression.

### Luciferase reporter assay

The transcriptional activity of YAP was detected as outlined in previous reports.<sup>22</sup> Briefly, HCC cells were co-transfected with 8xGTIIIC-luciferase plasmid and  $\beta$ -gal plasmid (Ambion, USA) using Lipofectamine<sup>TM</sup>2000 followed by ligustilide exposure. Approximately 72 h later, the activity of luciferase was determined using a Luciferase Reporter Assay Kit (BioVision, Milpitas, CA, USA). The activity of  $\beta$ -Gal was defined as a standard control for luciferase activity. All protocols were carried out according to the standard instructions.

### Statistical analysis

Data in this research were analyzed using the SPSS19.0 software and are shown as mean  $\pm$  SD of three or more independent experiments. Statistical comparisons were conducted using Student's *t*-test, ANOVA with *post hoc* Student–Newman–Keuls tests. The criterion for statistical significance was  $P < 0.05$ .

## Results

### Ligustilide counteracts cell proliferation and migration in HCC cells but has little cytotoxicity to normal hepatocytes

Prior to investigation of the function of ligustilide in HCC, its cytotoxicity to normal hepatocytes was determined. As shown in Figure 1(b), exposure to ligustilide at concentrations ranging from 0 to 200  $\mu$ M presented little toxicity on cell viability of normal HL-7702 hepatocytes. Further analysis substantiated that treatment with ligustilide dramatically restrained cell viability in HepG2 HCC cells in a dose-dependent manner; nevertheless, there was no obvious difference between 100- and 200  $\mu$ mol/L-treated groups (Figure 1(c)). Concomitantly, 100  $\mu$ mol/L of ligustilide suppressed the protein levels of proliferation-related Ki67 (Figure 1(d)). In parallel to these results, increased apoptosis in HCC cells was also validated after ligustilide treatment (Figure 1(e)). Additionally, cell migration ability was inhibited following ligustilide administration (Figure 1(f)).

### The ability of cancer cells to recruit and skew macrophages toward M2 phenotype is inhibited by ligustilide

To elaborate on the involvement of ligustilide in TME, we first investigated its efficacy on macrophage recruitment and polarization under the influence of cancer cells. Here, ligustilide treatment notably impaired the ability of HCC cells to recruit PMA-primed macrophages (Figure 2(a)). Importantly, HCC cell co-culture elevated the positive ratio of CD14<sup>+</sup>CD206<sup>+</sup> cells in THP-1 macrophages, which was attenuated after ligustilide treatment (Figure 2(b)). Moreover, stimulation of HCC cells with ligustilide reduced the mRNA levels of macrophage M2 phenotype markers, including CD163 (Figure 2(c)), CD206, CCL22, and Arg1 (Figure 2(d)). Analogously, ligustilide impeded co-culture-evoked transcripts and production of M2 macrophage marker TGF- $\beta$  and IL-10 (Figure 2(e) and (f)). Thus, ligustilide may interdict M2 macrophage induction ability under HCC cell conditions.

### Administration with ligustilide restrains nuclear translocation and activation of YAP

As shown in Figure 3(a), ligustilide administration decreased the mRNA levels of YAP in HCC cells. Moreover, ligustilide impeded 8xGTIIIC-luciferase activity (Figure 3(b)) and expression of the downstream effector of YAP, CTGF (Figure 3(c)), and indicating inhibitory effects on the transcriptional activity of YAP. Simultaneously, the accumulation of YAP protein in nucleus of HCC cells was decreased after ligustilide treatment (Figure 3(d)). It is known that phosphorylation of YAP can suppress nuclear translocation of YAP and its transactivation. Here, ligustilide treatment decreased total YAP protein levels and increased the levels of phosphorylated YAP protein (Figure 3(e)).

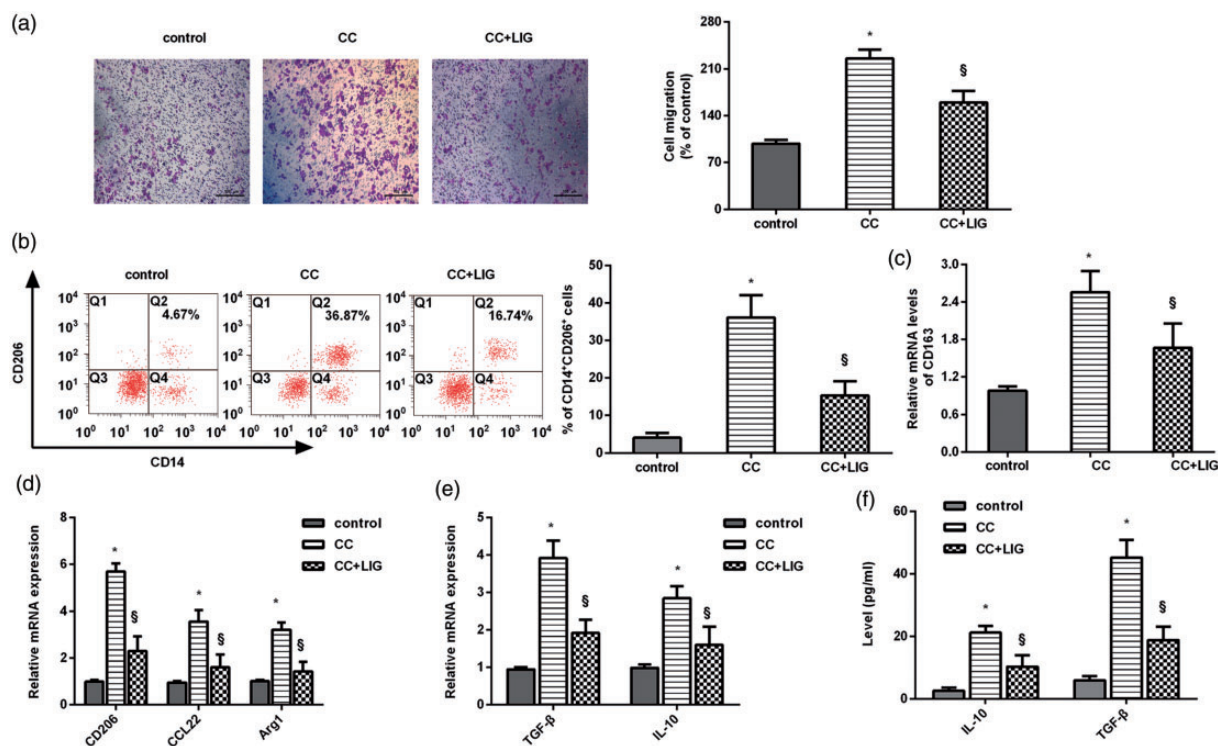


**Figure 2.** The ability of HCC cells to induce macrophage recruitment and M2 polarization was abrogated by ligustilide. (a) HCC cells under ligustilide exposure, or not, were co-cultured with PMA-treated THP-1 macrophages using the Transwell co-culture system. Macrophage migration was then analyzed. Macrophages without any treatment were defined as a control group. Scale bars, 100  $\mu$ m. (b) Flow cytometry was used to detect the percentage of CD14<sup>+</sup>CD206<sup>+</sup> cells in macrophages. (c and d) The mRNA levels of M2 macrophage phenotype markers were determined by qRT-PCR. (e and f) The transcript (e) and release (f) of M2 macrophage marker IL-10 and TGF- $\beta$  were further explored. \* $P < 0.05$  vs. control group.  $\$P < 0.05$  vs. CC-treated group. (A color version of this figure is available in the online journal.)

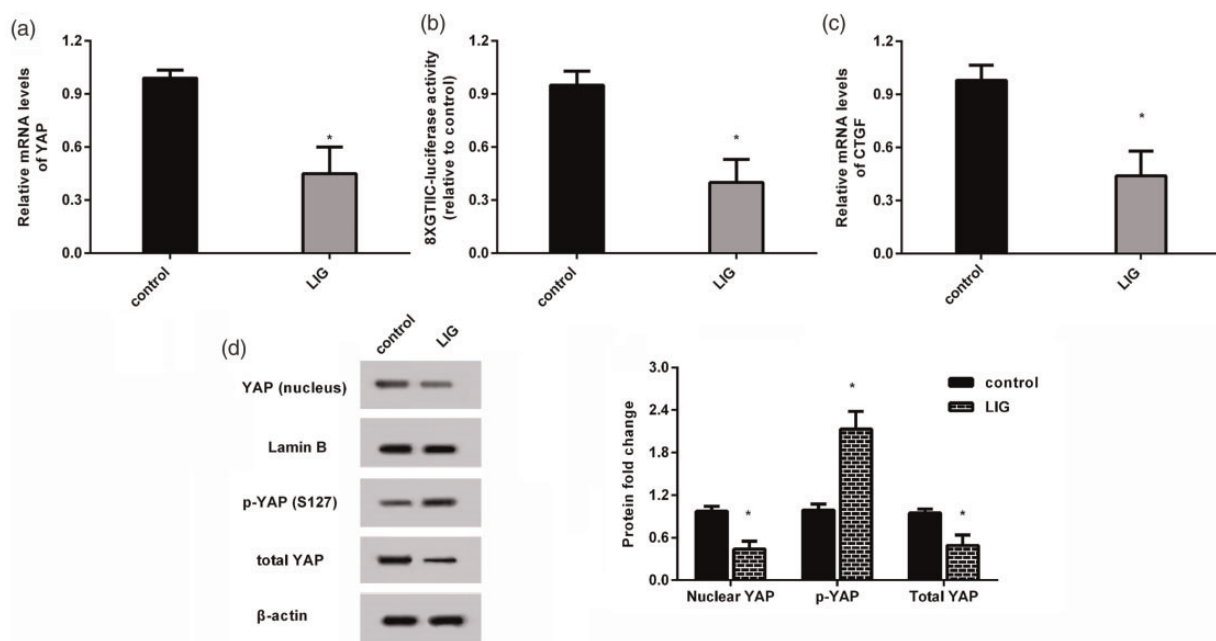


**Figure 3.** Ligustilide restrained nuclear translocation and activity of YAP in HCC cells. (a) The mRNA levels of YAP were detected in HCC cells after ligustilide treatment by qRT-PCR. (b) Then, luciferase activity of 8xGTIIc was applied to measure the transcriptional activity of YAP. (c) The expression of CTGF was determined. (d) The protein levels of YAP in nucleus were analyzed by Western blotting. (e) Total YAP and p-YAP protein levels were also measured. \* $P < 0.05$ .

**Elevation of YAP counteracts ligustilide-mediated inhibition of macrophage recruitment and polarization towards M2 phenotype induced by HCC cells**

Transfection with recombinant YAP plasmid dramatically elevated the mRNA (Figure 4(a)) and protein levels of YAP (Figure 4(b)) in HCC cells. Functional analysis substantiated that ligustilide treatment mitigated HCC cell co-culture-evoked macrophage recruitment, which was reversed after YAP overexpression (Figure 4(c)). Additionally, reactivating YAP signaling overturned the inhibitory efficacy of ligustilide on a co-culture-induced positive percentage of CD14<sup>+</sup>CD206<sup>+</sup> macrophages (Figure 4(d)). Concomitantly, the expression of M2 macrophage markers was increased after YAP overexpression relative to that of macrophages co-cultured with ligustilide-treated HCC cells, including CD163, CCL22, Arg1 and CD206 (Figure 4(e)), TGF-β and IL-10 (Figure 4(f)).

**Release of IL-6 by YAP in HCC cells is responsible for ligustilide-mediated macrophage recruitment and M2 polarization**

Further analysis revealed that ligustilide reduced the levels of IL-6 mRNA (Figure 5(a)) and release (Figure 5(b)) in HCC cells. Nevertheless, these decreases were reversed after YAP overexpression (Figure 5(a) and (b)), indicating that ligustilide may suppress IL-6 release in HCC cells by interdicting YAP. Importantly, inhibition of IL-6 by its antibody noticeably offset the suppressive effect on macrophage recruitment triggered by ligustilide-stimulated HCC cells (Figure 5(c)). Moreover, incubation with IL-6 antibody resulted in declines in the percentage of CD14<sup>+</sup>CD206<sup>+</sup> cells (Figure 5(d)), expression of CD206, CD163, CCL22, Arg1 (Figure 5(e)), and production of

IL-10 and TGF-β (Figure 5(f)) in macrophages co-cultured with HCC cells under ligustilide exposure. Intriguingly, additional supplementation with IL-6 reversed the inhibition effect of ligustilide on HCC cell-induced macrophage recruitment and M2 polarization (Figure 5(c) to (f)).

**Inhibition of IL-6R-STAT3 signaling by ligustilide accounts for macrophage M2 polarization evoked by IL-6 release from HCC cells**

Accumulating evidence has implicated IL-6 signaling in tumor-macrophage polarization and carcinogenesis in several cancers.<sup>23,24</sup> As shown in Figure 6(a) and (b), macrophages co-cultured with HCC cells exhibited higher protein levels of IL-6R and p-STAT3. However, HCC cells treated with ligustilide restrained the activation of IL-6R-STAT3 signaling in macrophages. Of interest, cessation of IL-6R expression muted the IL-6R-STAT3 pathway (Figure 6(c) and (d)). Moreover, IL-6 enhanced co-culture-induced macrophage migration (Figure 6(e)) and the percentage of CD14<sup>+</sup>CD206<sup>+</sup> cells (Figure 6(f)), and these effects were muted by blocking the IL-6R signaling. Additionally, si-IL-6R transfection in macrophages reduced IL-6-induced mRNA expression of Arg1, CD206, CD163, CCL22 (Figure 6(g)), IL-10, and TGF-β (Figure 6(h)), and production of IL-10 and TGF-β (Figure 6(i)) when cells were co-cultured with HCC cells.

**Discussion**

Recently, HCC is the second most prevalent aggressive liver tumor after hepatoblastoma and constitutes one of the most lethal cancer-related malignant carcinomas worldwide.<sup>2,3</sup> In the present study, we highlighted a key finding that ligustilide suppressed carcinogenesis of HCC cells by

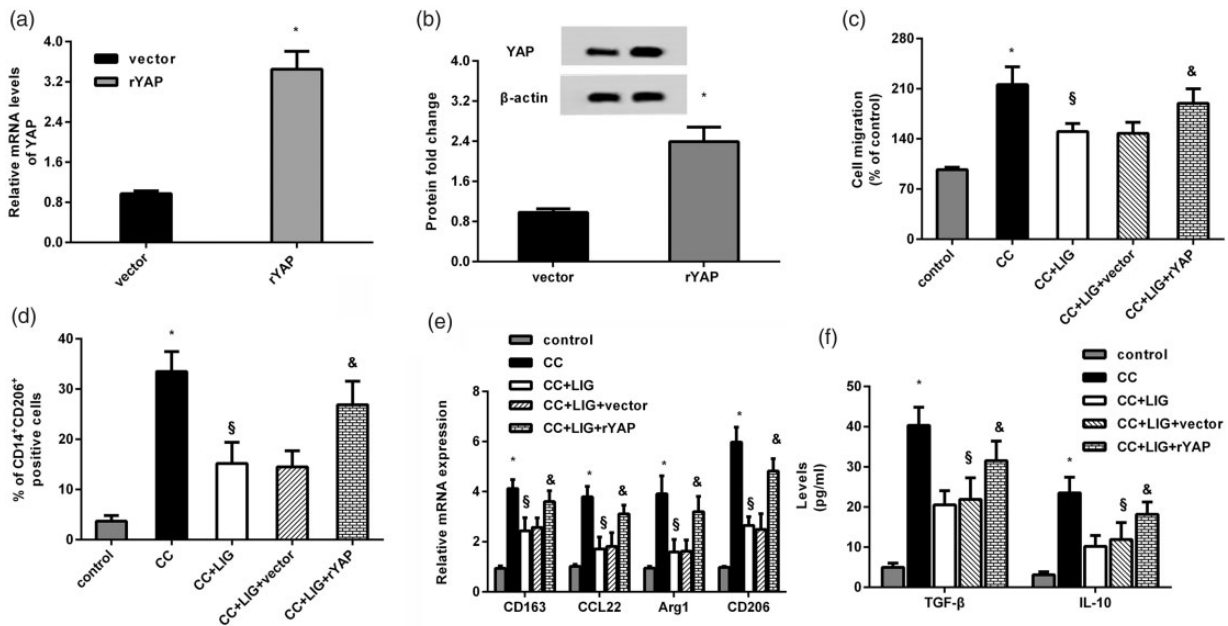


**Figure 4.** YAP involves in the inhibitory efficacy of ligustilide against HCC cell-induced macrophage recruitment and polarization towards M2 phenotype. (a and b) HCC cells were transfected with the recombinant rYAP plasmids, and the effects on YAP mRNA and protein levels were evaluated. (c to f) HCC cells transfected with rYAP vectors were treated with ligustilide, and co-cultured with macrophage. Then, cell migration (c), % of CD14<sup>+</sup>CD206<sup>+</sup> cells (d), mRNA levels of CD163, CCL22, Arg1, CD206 (e), and production of IL-10 and TGF-β (f) were assessed. \*P < 0.05 vs. control group. §P < 0.05 vs. CC-treated group. &P < 0.05 vs. CC and LIG group.

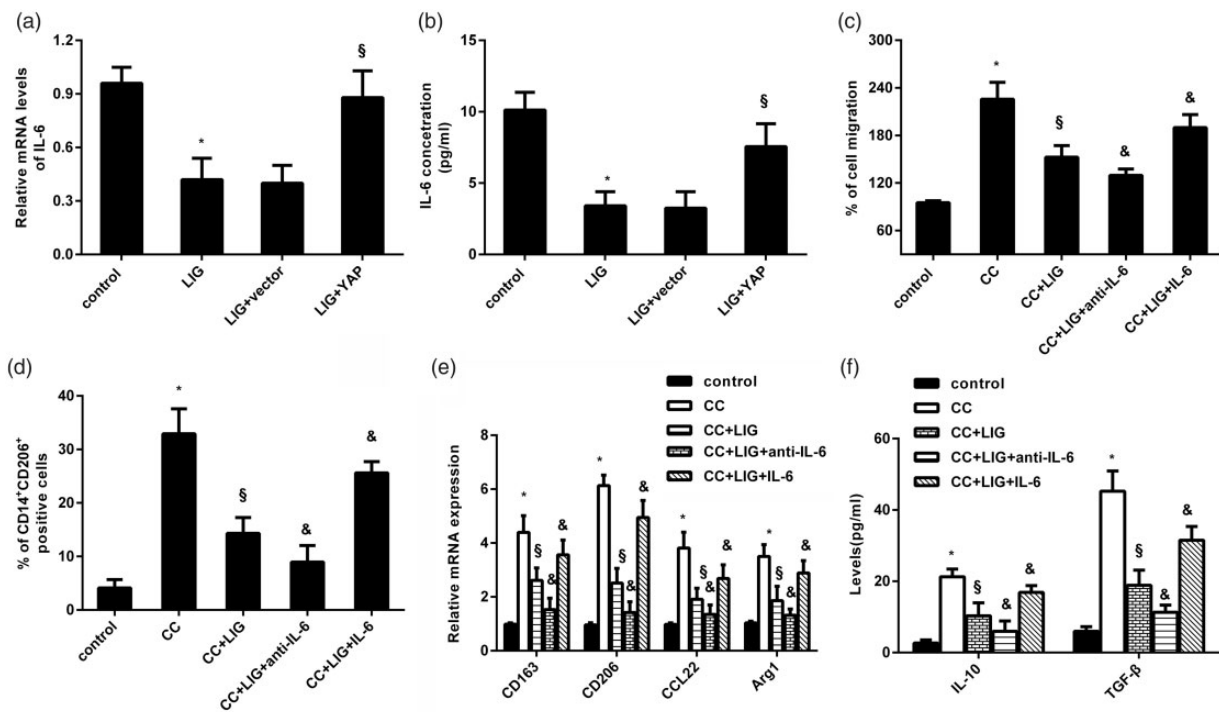


**Figure 5.** IL-6 secretion by YAP in HCC cells accounted for ligustilide-mediated macrophage recruitment and M2 polarization. (a and b) HCC cells were transfected with rYAP plasmids, prior to exposure to ligustilide. Then, the mRNA levels (a) and the contents of IL-6 in supernatants (b) were determined. (c and d) HCC cells stimulated with ligustilide, anti-IL-6 antibody, or exogenous IL-6 were co-cultured with macrophages. Then, macrophage migration (c) and % of CD14<sup>+</sup>CD206<sup>+</sup> cells (d) were analyzed. (e and f) The subsequent effects on the transcripts of CD163, CD206, Arg1, CCL22 (e), and production of IL-10 and TGF-β (f) were further evaluated. \**P* < 0.05 vs. control group. \$*P* < 0.05 vs. CC-treated group. &*P* < 0.05 vs. CC and LIG group.

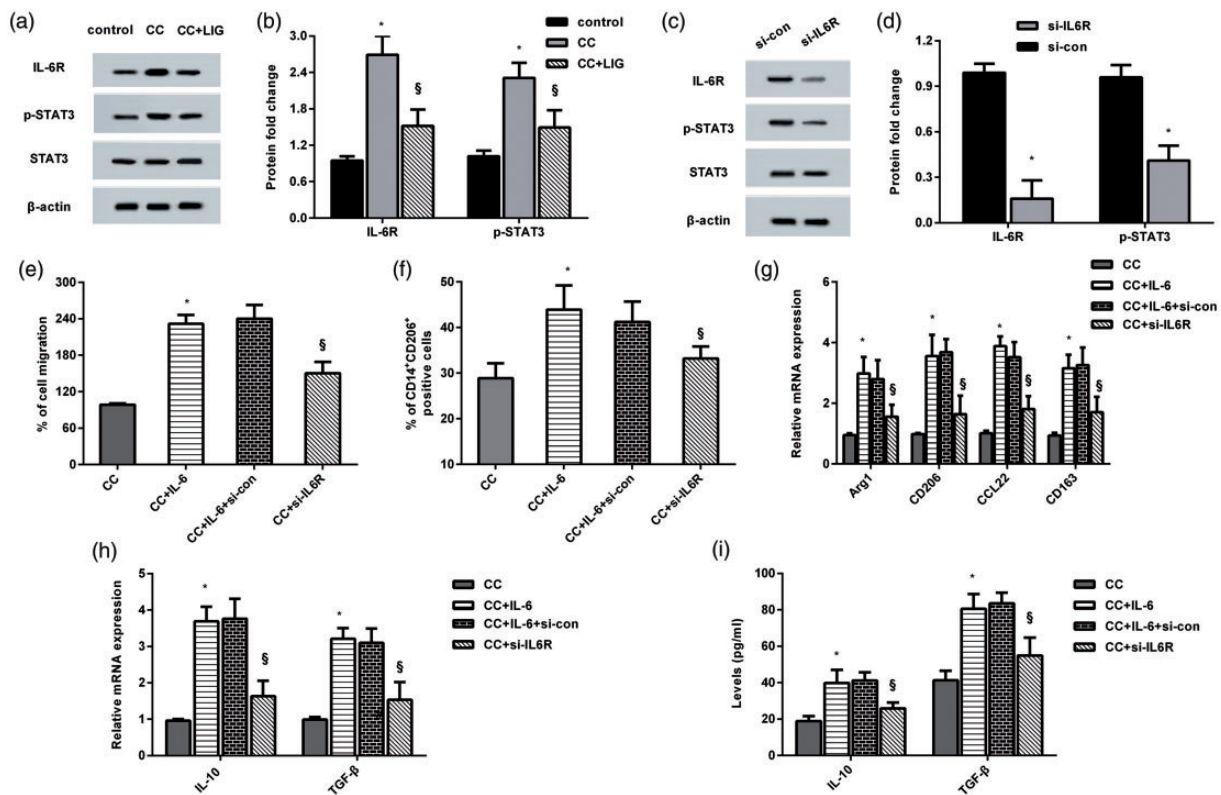


**Figure 6.** Blocking the IL-6R-STAT3 signaling by ligustilide involved in HCC cell co-culture-induced macrophage recruitment and M2 polarization evoked by IL-6 release. (a and b) After co-culture with HCC cells treated with ligustilide, the protein levels of IL-6R, p-STAT3, and STAT3 were analyzed. (c and d) After transfection with si-IL-6R, the activation of IL-6R/STAT3 signaling was detected. (e to i) Macrophages transfected with si-IL6R were co-cultured with HCC cells exposed to IL-6 conditions. Afterward, cell migration (e), % of CD14<sup>+</sup>CD206<sup>+</sup> cells (f), transcripts of CD206, Arg1, CCL22, CD163 (g), and the transcripts (h) and release (i) of IL-10 were monitored. \**P* < 0.05 vs. CC group. \$*P* < 0.05 vs. CC and IL-6 treated group.

inhibiting cell viability and migration. More importantly, ligustilide restrained HCC cell co-culture-evoked macrophage recruitment and M2 polarization by regulating activation of IL-6R-STAT3 signaling via YAP-induced IL-6 secretion. Consequently, this study may highlight a promising therapeutic agent for HCC by regulating cancer cell malignancy and cancer cell-mediated macrophage polarization within the TME.

Ligustilide fulfills pleiotropic pharmacological functions, such as anti-inflammation and anti-brain injury.<sup>15,16</sup> Intriguingly, the anti-tumor function of ligustilide has become a hotspot of research in the last few decades. In ovarian cancer, ligustilide exerts anti-apoptotic efficacy.<sup>17</sup> Similarly, the suppressive function of ligustilide in cell proliferation has been confirmed in non-small cell lung cancer.<sup>25</sup> It is worth mentioning that ligustilide exhibited little cytotoxicity to normal hepatocytes before we sought to investigate its function in HCC. Of interest, ligustilide restrained cell proliferation and migration but enhanced cell apoptosis in HCC cells. Analogously, a previous study corroborated that ligustilide impeded glioblastoma cell mobility.<sup>20</sup> Consequently, ligustilide may suppress the progression of HCC by directly affecting cancer cell growth and migration.

Increasing evidence has supported TME as a key and essential intrinsic portion for cancer initiation, development, and ultimately prognosis, including HCC.<sup>7,8</sup> Usually, tumor cells can constantly interact with surrounding stromal cells in the TME to regulate the progression of HCC.<sup>6</sup> Tumor-associated macrophages constitute the major components in TME and are associated with poor prognosis of patients with HCC.<sup>14</sup> After recruitment into the TME, macrophages will polarize into anti-tumor M1 or pro-tumor M2 phenotypes in response to factors secreted from carcinoma cells. It is a fact that cancer cells can promote M2 polarization of tumor-associated macrophages that will further facilitate tumor survival, growth, and metastasis.<sup>7,26,27</sup> Analogously to the previous study,<sup>12,26</sup> HCC cells could evoke macrophage recruitment and subsequent polarization to M2 phenotype. Importantly, we corroborated an interesting finding that ligustilide engendered the suppression in HCC cell-induced recruitment and M2 polarization of macrophages. Currently, an increasing body of evidence has suggested that targeting macrophage polarization towards M2 phenotype could complement the traditional therapeutic approach and improve therapeutic outcomes for these malignancies.<sup>13,14</sup> Therefore, ligustilide may affect the development of HCC by regulating the cross-talk between cancer cells and macrophages within the TME.

Further experiment corroborated the suppression of YAP activation by ligustilide in HCC cells by decreasing YAP nuclear expression, transcriptional activity and increasing p-YAP expression that can prevent YAP translocating to nucleus and inhibit its transactivation.<sup>28,29</sup> YAP is overexpressed in HCC patients, and its activity is elevated during the progression of liver carcinoma.<sup>30</sup> Noticeably,

YAP activation aggravates carcinogenesis by regulating tumor cell proliferation, chemoresistance, and metastasis.<sup>29,31</sup> Emerging evidence confirms the increasing attention on the relation between YAP activation and macrophage polarization in the development of carcinoma.<sup>32</sup> In HCC, enhancement of YAP expression promotes macrophage M2 polarization, and ultimately fosters HCC progression.<sup>26</sup> Additionally, YAP facilitates macrophage recruitment in HCC cells.<sup>12</sup> Our current data substantiated that YAP elevation counteracted the inhibitory effects of ligustilide on HCC-induced macrophage recruitment and M2 polarization. Noticeably, antagonizing the YAP oncogenic pathway can attenuate M2 tumor-associated macrophages, leading to the suppression of colon tumorigenesis.<sup>33</sup>

Mechanistically, ligustilide inhibited IL-6 production in a YAP-dependent manner in HCC cells. Importantly, a previous study confirmed that YAP induced IL-6 release that enhanced tumor-associated macrophage recruitment.<sup>12</sup> IL-6 is a common pro-inflammatory cytokine and can be produced by various cells, including tumor cells, and macrophages.<sup>12,24</sup> IL-6 has been implicated as a potential stimulator to regulate monocytic cell migration.<sup>34</sup> Accumulating evidence has proved that IL-6 intermediates macrophage polarization and oncogenesis by binding to IL-6R to activate the STAT3 signaling.<sup>24,35</sup> Here, IL-6 released from HCC cells further activated the IL-6R-STAT3 pathway in macrophages. Especially, the suppressive effects of ligustilide on macrophage recruitment and M2 polarization were further aggravated after IL-6 antibody incubation and were reversed after exogenous IL-6 treatment. Noticeably, IL-6 addition enhanced macrophage recruitment and M2 polarization, which was overturned by IL-6R/STAT3 signaling blockade. Analogously to this result, production of IL-6 from triple-negative breast cancer cells also facilitates M2 macrophage polarization by activating the IL-6R signaling.<sup>24</sup> Additionally, targeting IL-6 to regulate macrophage M2 polarization in TME may be a novel therapeutic strategy for colorectal cancer.<sup>23</sup>

## Conclusions

The current research highlighted a clear perspective that ligustilide could directly affect HCC cell survival and migration. Additionally, ligustilide suppressed HCC cell-induced macrophage recruitment and M2 polarization by inhibiting the IL-6R/STAT3 signaling via blockage of YAP-mediated IL-6 release from HCC cells. These findings suggest that ligustilide may attenuate the progression of HCC by regulating cancer cell malignancy and the interplay between tumor cells and macrophages in the TME. Consequently, this study supports that ligustilide may be a potential therapeutic agent that can complement and optimize the available therapeutic strategy for HCC.

## AUTHORS' CONTRIBUTIONS

All authors participated in the design, interpretation of the studies. JKY conducted cell culture, apoptosis, macrophage polarization, and qRT-PCR analysis. ZYX performed the Western blotting, cell migration, ELISA, and other experiments. ZYX analyzed the data and wrote the manuscript. All authors read and approved the final manuscript.

## DECLARATION OF CONFLICTING INTERESTS

The author(s) declared no potential conflicts of interest with respect to the research, authorship, and/or publication of this article.

## FUNDING

The author(s) received no financial support for the research, authorship, and/or publication of this article.

## ORCID iD

Zhiyuan Xing  <https://orcid.org/0000-0003-1082-2043>

## REFERENCES

- Bray F, Ferlay J, Soerjomataram I, Siegel RL, Torre LA, Jemal A. Global cancer statistics 2018: GLOBOCAN estimates of incidence and mortality worldwide for 36 cancers in 185 countries. *CA Cancer J Clin* 2018;**68**:394–424
- Cervello M, Emma MR, Augello G, Cusimano A, Giannitrapani L, Soresi M, Akula SM, Abrams SL, Steelman LS, Gulino A, Belmonte B, Montalto G, McCubrey JA. New landscapes and horizons in hepatocellular carcinoma therapy. *Aging* 2020;**12**:3053–94
- Kulik L, El-Serag HB. Epidemiology and management of hepatocellular carcinoma. *Gastroenterology* 2019;**156**:477–91 e1
- Sayiner M, Golabi P, Younossi ZM. Disease burden of hepatocellular carcinoma: a global perspective. *Dig Dis Sci* 2019;**64**:910–7
- Yarchoan M, Xing D, Luan L, Xu H, Sharma RB, Popovic A, Pawlik TM, Kim AK, Zhu Q, Jaffee EM, Taube JM, Anders RA. Characterization of the immune microenvironment in hepatocellular carcinoma. *Clin Cancer Res* 2017;**23**:7333–9
- Hui L, Chen Y. Tumor microenvironment: sanctuary of the devil. *Cancer Lett* 2015;**368**:7–13
- Lu C, Rong D, Zhang B, Zheng W, Wang X, Chen Z, Tang W. Current perspectives on the immunosuppressive tumor microenvironment in hepatocellular carcinoma: challenges and opportunities. *Mol Cancer* 2019;**18**:130
- Fu Y, Liu S, Zeng S, Shen H. From bench to bed: the tumor immune microenvironment and current immunotherapeutic strategies for hepatocellular carcinoma. *J Exp Clin Cancer Res* 2019;**38**:396
- Ruffell B, Affara NI, Coussens LM. Differential macrophage programming in the tumor microenvironment. *Trends Immunol* 2012;**33**:119–26
- Fu XL, Duan W, Su CY, Mao FY, Lv YP, Teng YS, Yu PW, Zhuang Y, Zhao YL. Interleukin 6 induces M2 macrophage differentiation by STAT3 activation that correlates with gastric cancer progression. *Cancer Immunol Immunother* 2017;**66**:1597–608
- Yeung OW, Lo CM, Ling CC, Qi X, Geng W, Li CX, Ng KT, Forbes SJ, Guan XY, Poon RT, Fan ST, Man K. Alternatively activated (M2) macrophages promote tumour growth and invasiveness in hepatocellular carcinoma. *J Hepatol* 2015;**62**:607–16
- Zhou TY, Zhou YL, Qian MJ, Fang YZ, Ye S, Xin WX, Yang XC, Wu HH. Interleukin-6 induced by Yap in hepatocellular carcinoma cells recruits tumor-associated macrophages. *J Pharmacol Sci* 2018;**138**:89–95
- Yang Y, Ye YC, Chen Y, Zhao JL, Gao CC, Han H, Liu WC, Qin HY. Crosstalk between hepatic tumor cells and macrophages via wnt/beta-catenin signaling promotes M2-like macrophage polarization and reinforces tumor malignant behaviors. *Cell Death Dis* 2018;**9**:793
- Mantovani A, Marchesi F, Malesci A, Laghi L, Allavena P. Tumour-associated macrophages as treatment targets in oncology. *Nat Rev Clin Oncol* 2017;**14**:399–416
- Liu X, Li X, Ji S, Cui X, Li M. Screening of bioactive ingredients in ligusticum chuanxiong hort for protection against myocardial ischemia. *Cell Physiol Biochem* 2016;**40**:770–80
- Kuang X, Wang LF, Yu L, Li YJ, Wang YN, He Q, Chen C, Du JR. Ligustilide ameliorates neuroinflammation and brain injury in focal cerebral ischemia/reperfusion rats: involvement of inhibition of TLR4/peroxiredoxin 6 signaling. *Free Radic Biol Med* 2014;**71**:165–75
- Lang F, Qu J, Yin H, Li L, Zhi Y, Liu Y, Fang Z, Hao E. Apoptotic cell death induced by Z-Ligustilide in human ovarian cancer cells and role of NRF2. *Food Chem Toxicol* 2018;**121**:631–8
- Ma H, Li L, Dou G, Wang C, Li J, He H, Wu M, Qi H. Z-ligustilide restores tamoxifen sensitivity of ERα negative breast cancer cells by reversing MTA1/IFI16/HDACs complex mediated epigenetic repression of ERα. *Oncotarget* 2017;**8**:29328–45
- Park Y, Kim D, Yang I, Choi B, Lee JW, Namkoong S, Koo HJ, Lee SR, Park MR, Lim H, Kim YK, Nam SJ, Sohn EH. Decursin and Z-Ligustilide in angelica tenuissima root extract fermented by *Aspergillus oryzae* display anti-pigment activity in melanoma cells. *J Microbiol Biotechnol* 2018;**28**:1061–7
- Yin J, Wang C, Mody A, Bao L, Hung SH, Svoronos SA, Tseng Y. The effect of Z-Ligustilide on the mobility of human glioblastoma T98G cells. *PLoS One* 2013;**8**:e66598
- Ma J, Mei J, Lu J, Wang Y, Hu M, Ma F, Long H, Qin Z, Tao N. Ligustilide promotes apoptosis of cancer-associated fibroblasts via the TLR4 pathways. *Food Chem Toxicol* 2020;**135**:110991
- Qin J, Shi H, Xu Y, Zhao F, Wang Q. Tanshinone IIA inhibits cervix carcinoma stem cells migration and invasion via inhibiting Yap transcriptional activity. *Biomed Pharmacother* 2018;**105**:758–65
- Chen L, Wang S, Wang Y, Zhang W, Ma K, Hu C, Zhu H, Liang S, Liu M, Xu N. IL-6 influences the polarization of macrophages and the formation and growth of colorectal tumor. *Oncotarget* 2018;**9**:17443–54
- Weng YS, Tseng HY, Chen YA, Shen PC, Al Haq AT, Chen LM, Tung YC, Hsu HM. 1/miR-34a/IL-6/IL-6R signaling axis promotes EMT progression, cancer stemness and M2 macrophage polarization in triple-negative breast cancer. *Mol Cancer* 2019;**18**:42
- Jiang X, Zhao W, Zhu F, Wu H, Ding X, Bai J, Zhang X, Qian M. Ligustilide inhibits the proliferation of non-small cell lung cancer via glycolytic metabolism. *Toxicol Appl Pharmacol* 2020;**410**:115336
- Zhao X, Wang X, You Y, Wen D, Feng Z, Zhou Y, Que K, Gong J, Liu Z. Nogo-B fosters HCC progression by enhancing Yap/taz-mediated tumor-associated macrophages M2 polarization. *Exp Cell Res* 2020;**391**:111979
- Huang WC, Kuo KT, Wang CH, Yeh CT, Wang Y. Cisplatin resistant lung cancer cells promoted M2 polarization of tumor-associated macrophages via the src/CD155/MIF functional pathway. *J Exp Clin Cancer Res* 2019;**38**:180
- Dong C, Wei KJ, Zhang WB, Sun H, Pan HY, Zhang L. LATS2 induced by TNF-alpha and inhibited cell proliferation and invasion by phosphorylating Yap in oral squamous cell carcinoma. *J Oral Pathol Med* 2015;**44**:475–81
- Dai XY, Zhuang LH, Wang DD, Zhou TY, Chang LL, Gai RH, Zhu DF, Yang B, Zhu H, He QJ. Nuclear translocation and activation of Yap by hypoxia contributes to the chemoresistance of SN38 in hepatocellular carcinoma cells. *Oncotarget* 2016;**7**:6933–47
- Perra A, Kowalik MA, Ghiso E, Ledda-Columbano GM, Di Tommaso L, Angioni MM, Raschioni C, Testore E, Roncalli M, Giordano S, Columbano A. Yap activation is an early event and a potential therapeutic target in liver cancer development. *J Hepatol* 2014;**61**:1088–96

31. Shi C, Cai Y, Li Y, Li Y, Hu N, Ma S, Hu S, Zhu P, Wang W, Zhou H. Yap promotes hepatocellular carcinoma metastasis and mobilization via governing cofilin/F-actin/lamellipodium axis by regulation of JNK/Bnip3/SERCA/CaMKII pathways. *Redox Biol* 2018;**14**:59–71
32. Yang W, Yang S, Zhang F, Cheng F, Wang X, Rao J. Influence of the Hippo-YAP signalling pathway on tumor associated macrophages (TAMs) and its implications on cancer immunosuppressive microenvironment. *Ann Transl Med* 2020;**8**:399
33. Huang YJ, Yang CK, Wei PL, Huynh TT, Whang-Peng J, Meng TC, Hsiao M, Tzeng YM, Wu AT, Yen Y. Ovatodiolide suppresses colon tumorigenesis and prevents polarization of M2 tumor-associated macrophages through Yap oncogenic pathways. *J Hematol Oncol* 2017;**10**:60
34. Clahsen T, Schaper F. Interleukin-6 acts in the fashion of a classical chemokine on monocytic cells by inducing integrin activation, cell adhesion, actin polymerization, chemotaxis, and transmigration. *J Leukoc Biol* 2008;**84**:1521–9
35. Yin Z, Ma T, Lin Y, Lu X, Zhang C, Chen S, Jian Z. IL-6/STAT3 pathway intermediates M1/M2 macrophage polarization during the development of hepatocellular carcinoma. *J Cell Biochem* 2018;**119**:9419–32

(Received December 20, 2020, Accepted March 26, 2021)